ANALYTIC SOLUTION OF THE ENVELOPE EQUATIONS FOR AN UNDEPRESSED MATCHED BEAM IN A QUADRUPOLE DOUBLET CHANNEL *

O. A. Anderson, LBNL, Berkeley, CA 94720, USA
L. L. LoDestro, LLNL, Livermore, CA 94551, USA

Abstract

In 1958, Courant and Snyder analyzed the problem of alternating-gradient beam transport and treated a model without focusing gaps or space charge. Recently we revisited their work and found the exact solution for matched-beam envelopes in a linear quadrupole lattice [O.A. Anderson and L.L. LoDestro, Phys. Rev. ST Accel. Beams, 2009]. We extend that work here to include the effect of asymmetric drift spaces. We derive the solution and show exact envelopes for the first two solution bands and the peak envelope excursions as a function of the phase advance σ up to $360°$. In the second stable band, decreased occupancy requires higher focusing strength. For symmetric gaps, this accentuates the remarkable compression effect predicted for the FD (gapless) model.

INTRODUCTION

In their classic paper, Courant and Snyder [1] studied the beam-envelope dynamics of a circular machine with negligible space charge, piecewise constant focusing, and no drift spaces (focusing gaps); they used an expansion in focusing strength to obtain an approximate solution for the matched envelope. The same case, but for a straight machine, was recently analyzed and an exact solution was obtained [2]. In the present paper we extend that recent analysis to include asymmetric focusing gaps, still assuming negligible space charge. Of course, particular cases with asymmetric gaps have long been studied via computer simulations; numerical examples with space charge are found in Refs. [3] and [4]. The motivations for finding the exact analytic envelope solution are: (1) performing parametric studies and studying the properties of the solutions such as extrema, limits, etc.; (2) facilitating study of envelope functions in the higher solution bands, where approximation methods fail and simulations become difficult. In particular, we are interested in the effect of drift spaces and asymmmetry on the remarkable second-band beam compression effect previously reported for the FD case [2].

Instead of solving the envelope equations directly, as we did in Ref. [2], we use here the linear single-particle equations and the phase-amplitude method to get the exact envelope functions and phase advances. To indicate briefly that, in our model, the periodic lattice of quadrupole doublets has piecewise-constant focusing but may have unequal gap lengths, we introduce the abbreviation $FoDO$.

* Supported in part by the U.S. Department of Energy under Contract No. DE-AC02-05CH11231.

FOCUSING MODEL

We assume a focusing function $\kappa(z)$ that is periodic over a lattice with period $2L$, so that $\kappa(z+2L) = \kappa(z)$. We take $\kappa(z)$ to be piecewise constant with value $+\kappa_{\max}$ in the focus and $-\kappa_{\max}$ in the defocus sections, which have equal length. For convenience throughout, we define

$$k \equiv \sqrt{\kappa_{\max}}\,. \tag{1}$$

Our FoDO model is then described for the xz-plane by Eqs. (2) and Fig. 1:

$$\kappa(z) \equiv \begin{cases} +k^2, & 0 < z < \eta L; \\ 0\,, & \eta L < z < \eta L + d_1; \\ -k^2, & \eta L + d_1 < z < 2\eta L + d_1; \\ 0\,, & 2L - d_2 < z < 2L. \end{cases} \tag{2}$$

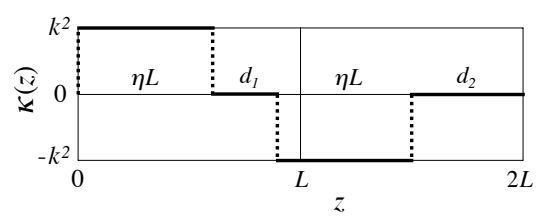

Figure 1: Model for xz-plane in one cell of a periodic FoDO lattice. The quadrupoles have equal lengths ηL; gap lengths are d_1 and d_2. The cell starts at $z = 0$ with $\kappa > 0$ (focus). The yz-plane field map is the same but inverted.

Since the FoDO lattice cell (Fig. 1) has equal focus and defocus lengths, the fields have antisymmetry about each gap center. For a matched beam, this yields a relationship between the envelopes $a(z)$ and $b(z)$ in the xz and yz planes, respectively. One finds that

$$b(z) = a(2z_c - z), \tag{3}$$

where z_c is the center of any gap. Therefore, we only need to analyze $a(z)$ in what follows.

DEFINITIONS

We define the *gap asymmetry parameter*

$$\mu \equiv \frac{d_2 - d_1}{2d}, \tag{4}$$

where

$$d \equiv \frac{d_2 + d_1}{2} = (1-\eta)L \tag{5}$$

so that

$$d_1 = d(1-\mu), \qquad d_2 = d(1+\mu). \tag{6}$$

The *normalized gap lengths* are

$$\nu \equiv kd = k(1-\eta)L = \tfrac{1-\eta}{\eta}\,\varphi, \quad (7)$$
$$\nu_1 \equiv kd_1 = \nu(1-\mu), \quad (8)$$
$$\nu_2 \equiv kd_2 = \nu(1+\mu). \quad (9)$$

The *focusing strength parameter*, used throughout this paper, is defined by

$$\varphi \equiv \eta k L. \quad (10)$$

We introduce the following quantities that depend on this parameter:

$$sn \equiv \sin\varphi, \qquad cs \equiv \cos\varphi,$$
$$sh \equiv \sinh\varphi, \qquad ch \equiv \cosh\varphi. \quad (11)$$

In the limit $\eta \to 1$, sn, cs, sh, and ch become identical with the functions defined in Ref. [2].

MATCHED BEAM ENVELOPES

For a beam with emittance $\in$, negligible space charge, and arbitrary periodic focus function $f(z)$, the xz-plane envelope function $a(z)$ is determined by [5]:

$$a(z)'' + f(z)a - \frac{\in^2}{a^3} = 0 \quad (12)$$

along with initial or periodic conditions for x and y. We assume $\in_x = \in_y = \in$. Without space charge, the beam distribution may be KV or a class of physically realistic distributions.

For a matched beam without space charge, it is unnecessary to solve the nonlinear equation (12) directly. Instead, we find the envelopes [6] using the phase-amplitude method [1], [4], which yields the result

$$\frac{1}{\in}a^2(z) = \frac{\mathbf{M}_{12}(z)}{\mathrm{P}\sqrt{1-(\frac{1}{2}\mathrm{Tr}\,\mathbf{M})^2}}, \quad (13)$$

with

$$\mathrm{P}(\varphi) \equiv \mathrm{sign}(\sin\varphi). \quad (14)$$

The function P provides the correct sign for the radical for any phase advance [2].

The matrix $\mathbf{M}$ is obtained by multiplying the transfer matrices for the segments of a lattice cell. In the case of a FoDO cell, these segments—taken in the order of Fig. 1—have transfer matrices [1], [7]

$$\mathbf{M}_F = \begin{pmatrix} cs & \frac{1}{k}sn \\ -k\,sn & cs \end{pmatrix}, \quad \mathbf{M}_{O_1} = \begin{pmatrix} 1 & d_1 \\ 0 & 1 \end{pmatrix},$$
$$\mathbf{M}_D = \begin{pmatrix} ch & \frac{1}{k}sh \\ k\,sh & ch \end{pmatrix}, \quad \mathbf{M}_{O_2} = \begin{pmatrix} 1 & d_2 \\ 0 & 1 \end{pmatrix}.$$

The matrix for the entire cell, starting at $z = 0$ in Fig. 1, is

$$\mathbf{M}(0) = \mathbf{M}(2L) = \mathbf{M}_{O_2}\mathbf{M}_D\mathbf{M}_{O_1}\mathbf{M}_F. \quad (15)$$

The ranges of z for the four individual segments are indicated in Fig. 1, namely, $\eta L, d_1, \eta L$, and d_2. If $z \neq 0$ but, for example, z lies within the first segment, then ηL and $\mathbf{M}_F$ split into ranges z and $\eta L - z$ as seen in Eq. (20).

Stability and Phase Advance σ

A single-particle orbit is stable if $2\cos\sigma = |\mathrm{Tr}\,\mathbf{M}| < 2$ [1]. We calculate the trace from $\mathbf{M}(0) = \mathbf{M}_{\mathrm{III}}\mathbf{M}_F$ where

$$\mathbf{M}_{\mathrm{III}} \equiv \mathbf{M}_{O_2}\mathbf{M}_D\mathbf{M}_{O_1} = \begin{pmatrix} A_1 & \frac{2B+sh}{k} \\ k\,sh & A_2 \end{pmatrix}, \quad (16)$$

$$A_1 \equiv ch + \nu_2\,sh, \qquad A_2 \equiv ch + \nu_1\,sh, \quad (17)$$

$$B \equiv \nu\,ch + \frac{1-\mu^2}{2}\nu^2 sh. \quad (18)$$

Then

$$\cos\sigma = \frac{\mathbf{M}_{11} + \mathbf{M}_{22}}{2} = (ch + \nu\,sh)cs - B\,sn \quad (19)$$

gives the phase advance, which agrees with the result given by Lund and Bukh [3]. The envelope solution will be stable for all values of φ for which the right-hand side of Eq. (19) lies within the range $[-1, 1]$. Such regions of φ or kL are referred to as pass bands. Reference [2] shows how these bands are related to the branches of $\cos\sigma$.

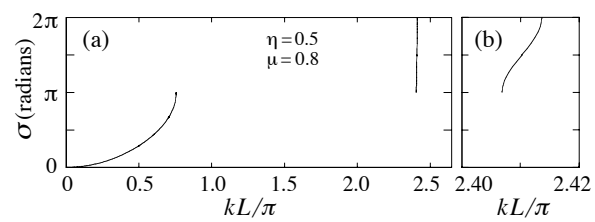

Figure 2: (a) Phase advance from Eq. (19) for the first two stable bands. (b) Band 2 with the kL axis magnified.

Exact Matched Beam Envelopes

For an arbitrary point z in the first (focus) segment, the transfer matrix is obtained from $\mathbf{M}_{\mathrm{III}}$ after pre- and post-multiplying by the two subunits of $\mathbf{M}_F$ referred to above.

$$\mathbf{M}^{\mathrm{f}}(z) = \begin{pmatrix} \cos kz & \frac{1}{k}\sin kz \\ -k\sin kz & \cos kz \end{pmatrix}\mathbf{M}_{\mathrm{III}} \times \begin{pmatrix} \cos k(\eta L - z) & \frac{1}{k}\sin k(\eta L - z) \\ -k\sin k(\eta L - z) & \cos k(\eta L - z) \end{pmatrix}. \quad (20)$$

The superscript "f" means that z is restricted here to the focusing segment. We define $F(\varphi, z) \equiv k\mathbf{M}^{\mathrm{f}}_{12}$ and find, with Eqs. (13) and (19), the exact focus-segment envelope:

$$a^2(\varphi, z) = \in\eta L\,\frac{F(\varphi, z)}{\mathrm{P}\varphi\sqrt{1-(\frac{1}{2}\mathrm{Tr}\,\mathbf{M})^2}} \quad (21)$$

$$F(\varphi, z) = (ch + \nu\,sh)sn + \mu\nu\,sh\sin[\varphi(1-2z/\eta L)] + B\,cs + (B + sh)\cos[\varphi(1-2z/\eta L)]. \quad (22)$$

There is no space here to present the exact solutions for all four segments—see Ref. [6]. Instead, we show the result for a complete cell graphically in Figs. 3 and 4. The lattice

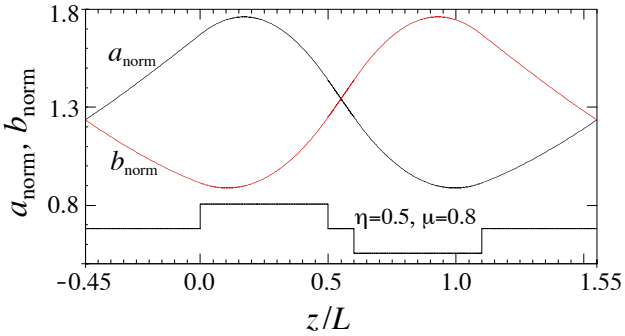

Figure 3: Envelope $a_{\rm norm} \equiv a(z)/\sqrt{\in L}$ from Eq. (21) and Ref. [6]. Focus parameter $kL = 0.60565\pi$ gives $\sigma = 80°$.

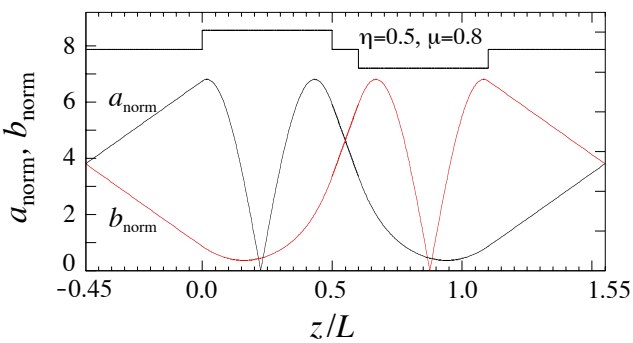

Figure 4: Same as Fig. 3 but with focus parameter $kL = 2.41027\pi$; $\sigma = 270°$, the middle of the second pass band.

parameters are $\eta = 0.5, \mu = 0.8$, with phase advances $\sigma = 80°$ and $\sigma = 270°$, respectively. Figure 3 uses the same parameters as in a numerical example by Lund et al. [4]. Our first-band envelopes are very like theirs (which include some space charge), but somewhat more compressed.

In the figures, $a(z)$ was obtained from our exact results, while $b(z)$ simply used Eq. (3). The origin has been shifted from that in Fig. 1. It is placed at the center of the second drift space in order to display the matched-beam symmetry described earlier.

Other Topics: peak excursion, beam compression

The peak value of the envelope determines whether the beam can pass through a given channel. There is an optimum value of the focus strength for each pass band, as seen in Fig. 5.

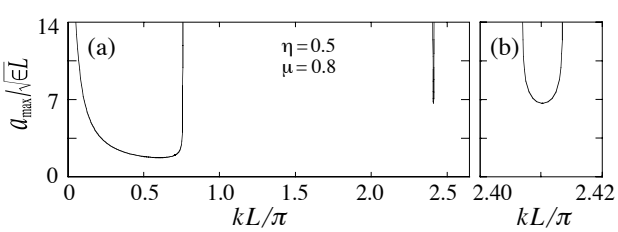

Figure 5: Peak envelope values taken from Ref. [6]. Same η and μ as in Figs. 2, 3, and 4. (a) First two stable bands. (b) Second band magnified.

Beam compression in even bands is due to envelope minima in the xz and yz planes occurring at or near the same z. Ref. [2] shows that the effect becomes extreme near the outer band edge (but it notes that caveats apply). The effect is even larger when there are drift spaces because the focusing strength must be increased. For $\eta = 0.5, \mu = 0.0$, and $\sigma = 356.75$, the area compression ratio is 1.17×10^6. However, if the asymmetry parameter μ is finite, the xz and yz compression points become separated and, for $\mu = 0.8$ (Fig. 6), the area compression ratio is only 7×10^4.

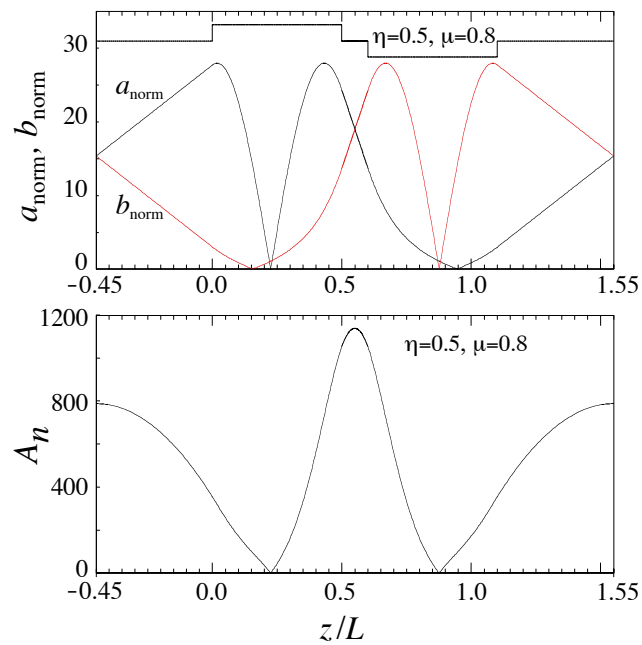

Figure 6: Normalized $a(z), b(z)$, and $A_n(z) \equiv \pi ab$ near outer edge of band 2: $kL = 2.41361\pi$; $\sigma = 356.6°$. The beam compression (7×10^4) is reduced because the gaps have unequal length and the $a(z)$ and $b(z)$ minima do not coincide—see text.

ACKNOWLEDGMENTS

We thank S.M. Lund and E.P. Lee for suggesting the transfer matrix method of solution.

REFERENCES

[1] E. D. Courant and H. S. Snyder, Ann. of Phys. **3**, 1 (1958).

[2] O. A. Anderson and L. L. LoDestro, Phys. Rev. ST Accel. Beams **12** (2009).

[3] S. M. Lund and B. Bukh, Phys. Rev. ST Accel. Beams **7**, 024801 (2004).

[4] S. M. Lund, S. H. Chilton, and E. P. Lee, Phys. Rev. ST Accel. Beams **9**, 064201 (2006).

[5] I. M. Kapchinskij and V. V. Vladimirskij, in *Conf. on High Energy Accel. and Instrum.* (CERN Sci. Inf. Service, Geneva, 1959), p. 274.

[6] O. A. Anderson and L. L. LoDestro, Tech. Rep. LBNL-1812E, Lawrence Berkeley Laboratory (2009).

[7] M. Reiser, Particle Accelerators **8**, 167 (1978).